Journal of Applied Polymer Science

Electric-field response behaviors of chitosan/barium titanate composite hydrogel elastomers

Ling-Xiang Gao,[1,2] Jian-li Chen,[1,2] Xue-Wu Han,[1,2] Jian-lan Zhang,[1,2] Shu-Xian Yan[1,2]

[1]Key Laboratory of Applied Surface and Colloid Chemistry (Ministry of Education), Shaanxi Normal University, Xi'an 710062, People's Republic of China

[2]School of Chemistry and Chemical Engineering, Shaanxi Normal University, Xi'an 710062, People's Republic of China

Correspondence to: L.-X. Gao (E-mail: gaolx@snnu.edu.cn)

ABSTRACT: Chitosan/barium titanate ($BaTiO_3$) composite hydrogel elastomers were prepared in the presence or absence of an applied direct-current (dc) electric field. Scanning electron microscopy was used to observe the microstructure of the elastomers and the dispersion of particles in it. Tests of the storage moduli (*G*s) of the elastomers were investigated with a dynamic mechanical analyzer. On this basis, the *G* increment and increment sensitivity were explored. The results show that the particles were sequentially dispersed, and the values of the *G* values for the elastomer were higher under an external applied dc electric field; this indicated that the composite elastomers exhibited excellent electric field response. Furthermore, the electric-field response of the composite elastomers changed with the particle concentration, and the maximum response occurred when the mass fraction of $BaTiO_3$ was 2.0%. The *G* value of the composite elastomer with a $BaTiO_3$ weight percentage of 2.0 increased with increasing electric field; this revealed that the composite elastomer had a positive electric field response. © 2015 Wiley Periodicals, Inc. J. Appl. Polym. Sci. **2015**, *132*, 42094.

KEYWORDS: composites; elastomers; rheology

Received 22 October 2014; accepted 10 February 2015

DOI: 10.1002/app.42094

INTRODUCTION

Electrorheological (ER) materials are typical composite soft matters that consist of semiconducting micrometer-sized particles and an insulating carrier matrix, which show a dramatic and reversible increase in their mechanical modulus when an electric field is applied. Because of their controllable electric properties in mechanics, electrics, and optics,[1–5] ER materials have many potential engineering applications, such as in sensing,[6,7] electronics,[8] damper systems,[9,10] and vibration controls.[11] ER elastomers, which are solidlike ER materials and are composed of dispersed particles in a chemical crosslinking network of organic macromolecules,[12,13] have recently attracted considerable attention in the research community.[14,15] Because of the matrix's solidlike nature of elastomers, particles are restricted, and their aggregations are eliminated. Consequently, the instability of the ER effect, which is caused by the particles' congregation in ER fluid, is improved.[14–16] At the same time, the interaction among the polarized particles under an applied electric field induces a change in the elasticity of the composite elastomer; this is known as the ER effect. On the basis of the ER effect, ER elastomers can be applied in several fields, including dampers, clutches in automotive industries, and smart skins in bionic technology.[17,18] However, most of them are synthetic polymer hydrogels, for example, poly(acrylate) copolymers, poly (dimethyl siloxane), poly(styrene butadiene), poly(styrene isoprene styrene), and silicone rubber,[19–21] whose poor biocompatibility and possible toxicity limit their applications in the field of biomedicine.[22,23] Natural biological macromolecules have attracted tremendous attention on account of their outstanding properties. It is possible to use natural biological macromolecule hydrogels in the biological medicine field because of its nontoxicity, good biocompatibility, and electric field sensitivity. Gao and Zhao[15] prepared a barium titanate ($BaTiO_3$)/gelatin composite ER elastomer and researched its favorable ER properties. However, the maximum elastic modulus increment sensitivity ($\Delta G/G_R$, where ΔG is the storage modulus increment, G_R is the storage modulus of the elastomer cured without electric field) was only 79.32% under the measured electric field of 1 kV/mm. In addition, Gao and Zhao[24] prepared starch/glycerin/gelatin hydrogel hybrid elastomers and found that the $\Delta G/G_R$ attained a maximum value of 21.04% at a measured electric field of 2 kV/mm. Until now, there have been only a few examples of biomolecular hydrogels as matrixes of ER elastomers, such as gelatin, which are limited in green, environmentally friendly properties and low cost in cost.[15,24–27] In these reported works, the main problem with the elastomer has been that the elastic

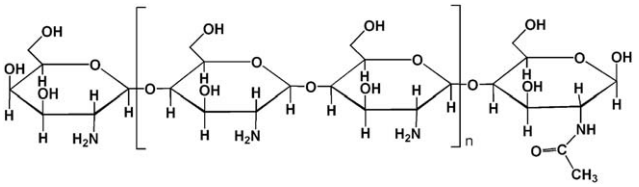

Figure 1. Chemical structure of CTS.

$\Delta G/G_R$ is too low. General studies on hydrogel matrixes have not yet been expanded. Chitosan (CTS; Figure 1) as a natural biomaterial is a nontoxic polysaccharide consisting of β-(1,4)-linked 2-deoxy-2-amino-*d*-glucopyranose units, which can be obtained by the alkaline hydrolysis of chitin, one of the most plentiful natural biopolymers in the world. Reactive —NH_2 and —OH on the hexatomic ring of CTS can effectively offer a convenient acquired elastomer with novel properties.[28,29]

On the basis of these studies, we prepared $BaTiO_3$/CTS composite hydrogel elastomers and study their electric-field response via freeze drying, scanning electron microscopy (SEM), and dynamic viscoelasticity analysis.

EXPERIMENTAL

Materials

Tetrabutyl titanate, barium hydroxide, formic acid, ethanol, ammonia acetonitrile, and so on were all analytical-reagent grade and were used as received without further purification. Glutaraldehyde solution (analytical-reagent grade, 50 wt %), as a crosslinking reagent, was diluted to 2 wt %. CTS $[(C_6H_{11}NO_4)_n]$, with a deacetylation degree of 80.0–95.0%, a viscosity of 50–800 mPa s, and an average molecular weight of 5.9×10^5, was purchased from Sinopharm Chemical Reagent Co., Ltd. Deionized water was used in all of the investigating processes.

Preparation of the $BaTiO_3$ Particles

$BaTiO_3$ particles were prepared in our laboratory according to the literature.[30] With ammonia–water solution, acetonitrile, and tetrabutyl titanate reacting in ethanol, the TiO_2 microsphere was gained. Then, the TiO_2 sphere was reacted with barium hydroxide in a Teflon autoclave reactor at 100°C for 24 h. After the sample was filtered, washed, and dried, $BaTiO_3$ particles were obtained.

Preparation of the $BaTiO_3$/CTS Composite Hydrogel Elastomers

A CTS/acetic acid solution with a concentration of 3 wt % was prepared via the dissolution of an amount of CTS in 2 wt % acetic acid solution at 60–70°C. Then, various weighed amounts of $BaTiO_3$ particles were dispersed in CTS/acetic acid solutions according to $BaTiO_3$ weight percentages (Φ_{BT}) of 0, 0.5, 1.0, 1.5, 1.75, 2.0, 2.25, 2.5, 3.0, 4.0, 6.0, 8.0, 10.0, 12.0, and 15.0. After the blend was stirred for about 30 min, an appropriate amount of chemical crosslinking agent (glutaraldehyde solution 4 wt %) was added, and it dispersed rapidly. The mechanism of chemical crosslinking that accounted for the action of glutaraldehyde is described as follows: Glutaraldehyde crosslinked with the amine group of the CTS molecule through an amine–aldehyde condensation reaction into a network structure (Figure 2).[31]

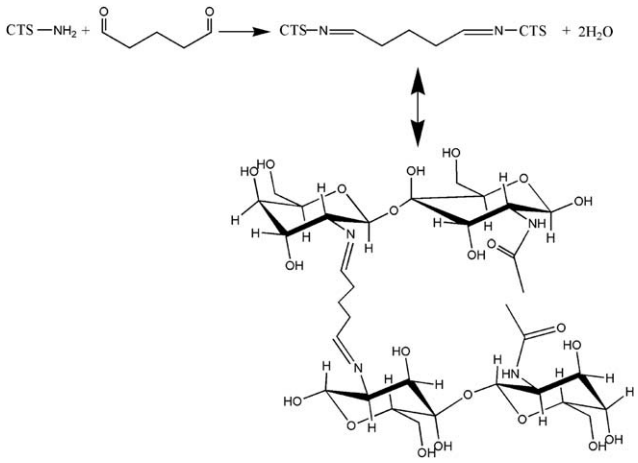

Figure 2. Mechanism of the crosslinking reaction of CTS and glutaraldehyde.

Then, the suspension was transferred quickly into two custom-made Plexiglas boxes simultaneously and cured synchronously with and without a parallel direct-current (dc) electric field (1 kV/mm). On the basis of lots of experimental results of the study of the electric field response of the CTS hydrogel, we found that the obvious response occurred until the electric field was increased to 1 kV/mm. Here, the Plexiglas boxes were equipped with two copper foils as electrodes, as illustrated in Figure 3. The dc electric fields were applied on the one box in the upright direction of the curing system at the beginning of the curing process with a high-voltage power (regulator range = 0–30 kV, Tianjin Dongwen High Voltage Power Factory). After 50 min, the electric field was withdrawn, and the temperature was continually maintained at 60–70°C for 1 h. Then, by a natural temperature decrease, the two elastomers

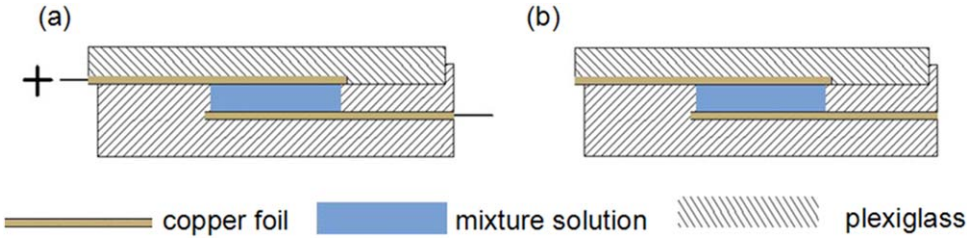

Figure 3. Side view of Plexiglas boxes for curing the two elastomers: (1) curing under the applied dc electric field and (2) curing without a field. [Color figure can be viewed in the online issue, which is available at wileyonlinelibrary.com.]

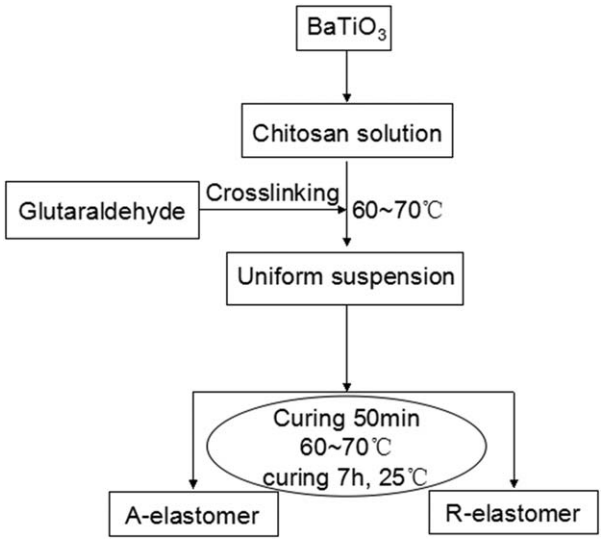

Figure 4. Flow chart of the preparation of the $BaTiO_3$/CTS composite elastomers.

were cured at 25°C for 7 h and were finally prepared. Here, the elastomer we call the *A* elastomer was cured under an electric field, and we call the elastomer cured without any field is the *R* elastomer. Figure 4 shows the preparation of the $BaTiO_3$/CTS composite elastomers in flow chart form.

Test and Characterization

SEM of the morphology and microstructure of the $BaTiO_3$ particles and the composite elastomers was performed with a Quanta 200 environmental scanning electron microscope with an energy dispersive spectrometer (EDS). X-ray diffraction (XRD) patterns were obtained with a D/Max-3c X-ray diffractometer with Kα radiation ($\lambda = 1.5406$ Å) at an operation voltage and current of 40 kV and 40 mA, respectively.

The storage modulus (*G*) is one of the important mechanical properties for elastomers; it was measured by a Q800DMA dynamic viscoelastic spectrometer (TA Instrument Co., Ltd.) in static-press multifrequency mode. The thickness of the sample specimens was typically 8 mm, and the diameter was about 12 mm. Each measurement was conducted with the frequency range 1–10 Hz at room temperature at an appropriate strain of 1.0%, and each *G* was determined from the average of at least four repeated data from different samples of the same elastomer.

RESULTS AND DISCUSSION

Morphology and Structure of the $BaTiO_3$ Particles

Figure 5 shows the SEM micrograph and XRD pattern of the prepared $BaTiO_3$ particles. SEM indicates that the $BaTiO_3$ particles were uniformly distributed symmetrical spherical particles, and their diameter was about 2–3 μm. The baseline of XRD was steady without artificial bands, and there was one single diffraction peak at $2\theta \approx 45°$ without splitting diffraction peaks; this confirmed that the $BaTiO_3$ particle was in a cubic crystal phase.[32,33]

Distribution of the $BaTiO_3$ Particles in the CTS Composite Elastomer

We used CTS hydrogel as the continuous phase (i.e., the matrix) and $BaTiO_3$ particles as the dispersed phase to prepare composite elastomers cured in the presence or absence of an applied dc electric field. To obtain detailed microstructure information about the morphology and composition of the $BaTiO_3$/CTS composite hydrogel elastomer, SEM was carried out with microflakes that had been freeze-dried at a thickness of less than 0.5 mm. Figure 6(a) shows the SEM of the *A* elastomer with $\Phi_{BT} = 2.0$, and Figure 6(b) shows that of the corresponding *R* elastomer. There is an obvious difference between Figure 6(a) and 6(b). In Figure 6(a), the particles are dispersed well in line in the direction of the applied electric field, and the matrix structure of the hydrogel exhibits clear linearity in the same direction. However, the particles are randomly dispersed, and the hydrogel structure appears nonlinear in Figure 6(b).

According to dielectric polarization theory,[14,16] $BaTiO_3$ particles are polarized under an applied field, and this can induce positive/negative charges on the opposite tips of the particles; this is referred to an *induced dipole*. An attractive interaction between the dipoles in the field direction causes the adjacent particles to draw near to each other. Meanwhile, a repulsive interaction between identical charges perpendicular to the field direction causes the equatorial particles to repel each other. The electrostatic forces also reduce the particle aggregation in the field

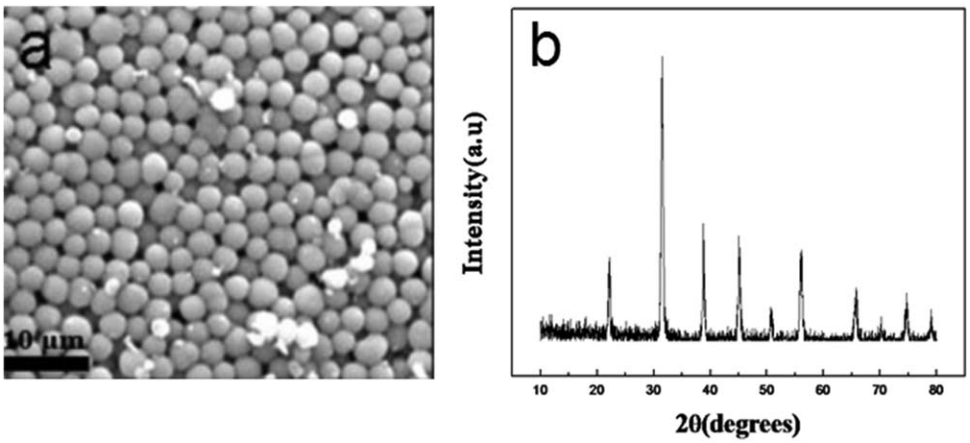

Figure 5. (a) SEM image of the $BaTiO_3$ samples and (b) XRD pattern of the $BaTiO_3$ samples on the diffraction peak with $2\theta = 20–80°$.

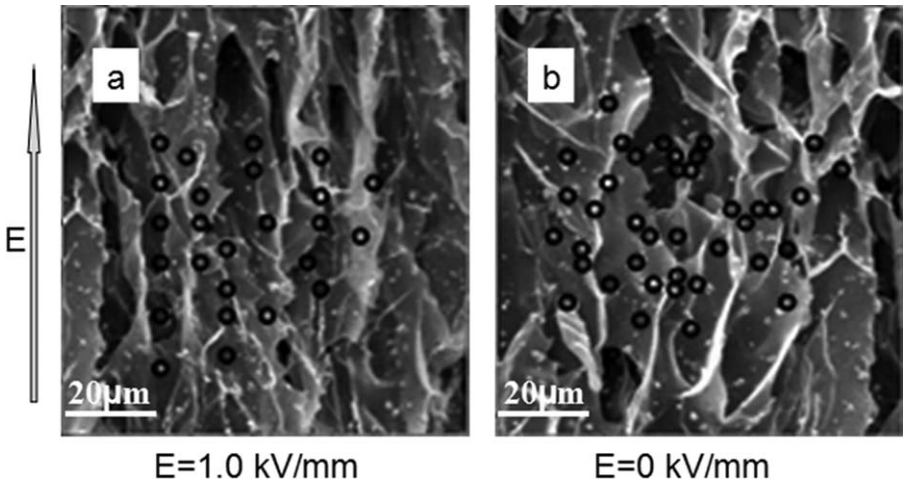

Figure 6. SEM images of the microstructure of (a) *A* elastomer (The dc electric field $E = 1.0$ kV/mm) and (b) *R* elastomer (The dc electric field $E = 0.0$ kV/mm).

direction, and these are like chains (so-called pearl chains). Synchronously, the particles' good chain aggregation brings the matrix network to linearity. By comparing and analyzing the two elastomers, we found that the particles were aligned by the applied dc field during the curing process, whereas the particles dispersed randomly without an applied field. The mechanism is depicted in Figure 7.

G Values of the $BaTiO_3$/CTS Composite Elastomers as a Function of the Weight Fraction of Particles

The *G* values of the *A* and *R* elastomers were measured as a function of Φ_{BT}, as shown in Figure 8. Along with increasing Φ_{BT}, the moduli of the *A* and *R* elastomers increased together; this was due to the particles' filler effect. Furthermore, *G* of the *A* elastomer was higher than that of the corresponding *R* elastomer, whose range was $0 < \Phi_{BT} < 15$. The main reason was probably a pearl-chain effect, in which the adjacent aligned particles of *A* elastomer in the field direction could resist stress better than the randomly distributed particles in the *R* elastomer.[14,15,34] When $\Phi_{BT} = 0$, the moduli of the *A* and *R* elastomers were almost the same, which was only due to their matrix, the CTS hydrogel. This phenomenon indicated that the pure CTS hydrogel did not respond to the applied electric field. When $\Phi_{BT} = 15$, the particles did not disperse well because of their heavy concentration in the elastomer. Consequently, the heavy weight made the particles in the *A* elastomer unable to align, and the pearl-chain effect could not be revealed. As also shown in Figure 8, the modulus of the *A* elastomer increased within the Φ_{BT} range of 0–2.0 decreased within the range 2.0–8.0, and then increased again when Φ_{BT} was greater than 8.0.

To clearly determine the effect of the electric field response performance of the gel as a function of Φ_{BT}, ΔG, and $\Delta G/G_R$ were treated as follows:

$$\Delta G = G_A - G_R$$

$$\Delta G/G_R = (G_A - G_R)/G_R$$

As shown in Figure 9(a), it was clear that ΔG increased with increasing Φ_{BT} between 0 and 2.0. Then, it decreased with increasing Φ_{BT} in the range 2.0–15.The peaks of ΔG appeared at a Φ_{BT} of 2.0. The peak modulus of the *A* elastomer (G_A) was

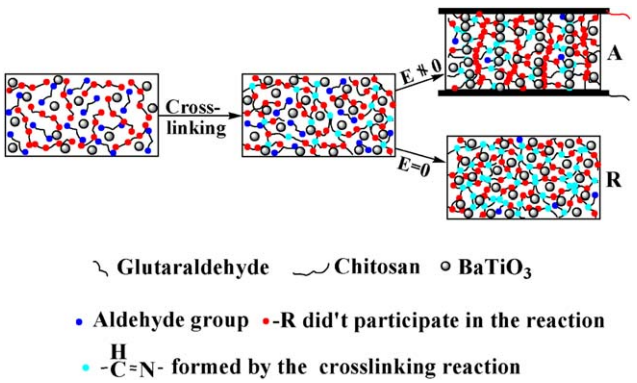

Figure 7. Structure of the composite gels in the presence or absence of electric fields. [Color figure can be viewed in the online issue, which is available at wileyonlinelibrary.com.]

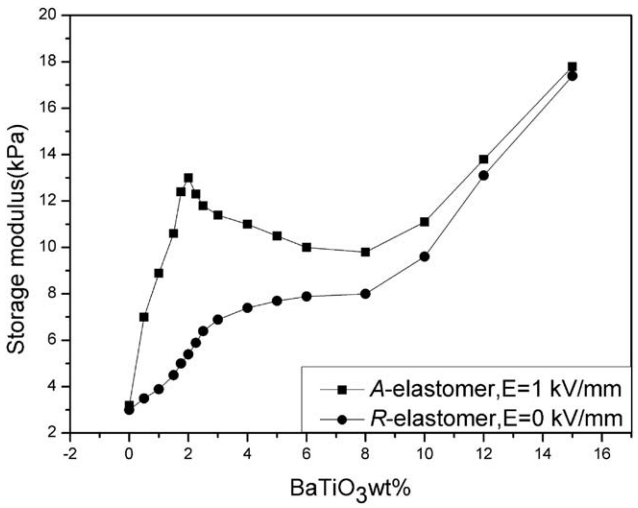

Figure 8. *G* values of the *A* elastomer and *R* elastomer as a function of Φ_{BT}.

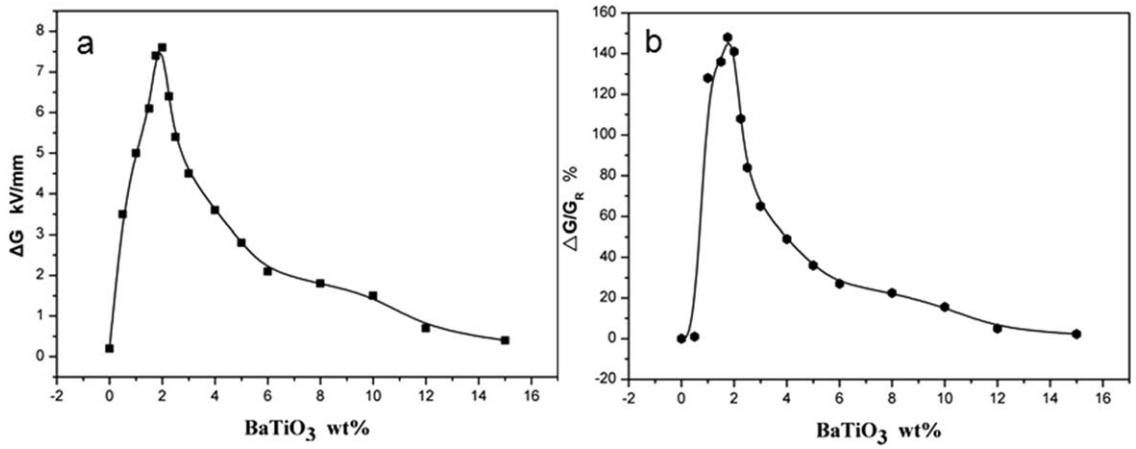

Figure 9. ΔG and $\Delta G/G_R$ as a function of Φ_{BT}.

13.0 kPa, whereas G_R of the corresponding *R* elastomer was 5.4 kPa. The ΔG ($\Delta G = G_A - G_R$) was 7.6 kPa.

Similar phenomena are shown in Figure 9(b). $\Delta G/G_R$ first increased and then decreased with increasing Φ_{BT} (from 0 to 15.0). The largest $\Delta G/G_R$ occurred at a Φ_{BT} of about 2.0, and $\Delta G/G_R$ was 140.8%.

This result suggests that the $BaTiO_3$/CTS composite elastomer possessed the strongest response to an electric field at $\Phi_{BT} = 2.0$, and the ultimate value of the response effect was 140.8%. The reason was that the particles dispersed uniformly and could easily form a chain under a field when Φ_{BT} was less than 2.0, and the chain acted as a major resistance to the load force. With increasing Φ_{BT}, both the pearl-chain effect and the filler effect grew stronger to promote the obvious increment in the modulus. When Φ_{BT} was greater than 2.0, the heavier concentration of particles enhanced the filler effect and weakened the chain effect because of increasing particle natural aggregation. Both the increasing filler effect and decreasing chain effect caused *G* of the *A* elastomer to decrease anteriorly and increase posteriorly with increased Φ_{BT}.[25,34] Concomitantly, the random particles in the *R* elastomer acted only as fillers, and the filler effect became stronger with increasing concentration of particles, so the modulus increased, depending on Φ_{BT}. Until Φ_{BT} was greater than 8.0, as the particles' heavy weight weakened the chain effect, the filler effect was the major force of the moduli of the *A* elastomer, so the moduli increased with the particles' weight fraction, in a manner similar to that of the *R* elastomer.

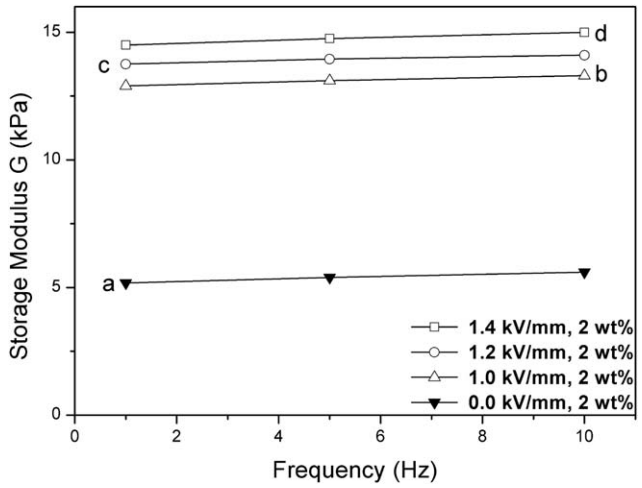

Figure 10. *G* values of the gel with $\Phi_{BT} = 2.0$ as a function of the electric field: (a) 0, (b) 1.0, (c) 1.2, and (d) 1.4 kV/mm.

G Value of the $BaTiO_3$/CTS Composite Elastomer as a Function of the Electric Field

Here, we measured *G* of the *A* elastomers ($\Phi_{BT} = 2.0$) with different electric fields, increasing from 0 to 1.4 kV/mm, as shown in Figure 10(a–d). We observed that *G* of the *A* elastomer increased with increasing applied electric field, and the higher electric field could cause a stronger response. This indicated that the $BaTiO_3$/CTS composite elastomer possessed a positive response to the electric field. The reason may have been that the stronger electric field enhanced the particles' pearl-chain effect and induced a higher *G* in the elastomer.

CONCLUSIONS

Response behaviors of the $BaTiO_3$/CTS hydrogel composite elastomers composed of CTS and $BaTiO_3$ were investigated. For the composite elastomer, $BaTiO_3$ particles were polarized and aligned when they were cured under an applied dc electric field, and their pear-chain effect induced a large elastomer *G* and a strong response to the field. ΔG of the composite elastomers was strongly affected by the $BaTiO_3$ particles' electric field response and its concentration. The $BaTiO_3$/CTS composite elastomer possessed a stronger response to an electric field of 1 kV/mm at $\Phi_{BT} = 2.0$ with an ultimate value of 140.8%; this was higher than that of the $BaTiO_3$/gelatin composite ER elastomers, and the response increased with increasing field strength.

ACKNOWLEDGMENTS

This work was supported by the National Natural Science Foundation of China (contract grant number 20941001).

REFERENCES

1. Tohru, S.; Takashi, O.; Yoshiharu, H.; Akane, O.; Toshio, K. *J. Mater. Sci.* **1993**, *28*, 1293.

2. Parthasarathy, M.; Klingenberg, D. J. *Mater. Sci. Eng.* **1996**, *R17*, 57.
3. Zrinyi, M.; Feher, J.; Filipcsei, G. *Macromolecules* **2000**, *33*, 5751.
4. Zhao, Q.; Zhao, P.; Qu, P.; Xiang, L. Q. *Appl. Phys. Lett.* **2004**, *84*, 1985.
5. Zhao, X. P.; Liu, S.; Tang, H.; Yin, J. B.; Luo, C. R. *J. Intell. Mater. Syst. Struct.* **2005**, *16*, 57.
6. Niu, X.; Zhang, M. Y.; Wu, J. B.; Wen, W. J.; Sheng, P. *Soft Matter* **2008**, *5*, 576.
7. Yarimaga, O.; Jaworski, J.; Yoon, B.; Kim, J.-M. *Chem. Commun.* **2012**, *48*, 2469.
8. Ohko, Y.; Tatsuma, T.; Fujii, T.; Naoi, K.; Niwa, C.; Kubota, Y.; Fujishima, A. *Nat. Mater.* **2003**, *2*, 29.
9. Choi, S.-B.; Han, Y.-M. *J. Sound Vibr.* **2007**, *303*, 391.
10. Yamaguchi, H.; Zhang, X.-R.; Niu, X.-D.; Nishioka, K. J. *Intell. Mater. Syst. Struct.* **2010**, *21*, 423.
11. Wei, K.; Bai, Q.; Meng, G.; Ye, L. *Smart Mater. Struct.* **2011**, *20*, 055012.
12. Shiga, T.; Okada, A.; Kurauchi, T. *Macromolecules* **1993**, *26*, 6958.
13. Hanaoka, R.; Takata, S.; Fujita, H.; Fukami, T.; Sakurai, K.; Iisobe, K.; Hino, T. *Int. J. Mod. Phys. B* **2002**, *16*, 2433.
14. Krause, S.; Bohon, K. *Macromolecules* **2001**, *34*, 7179.
15. Gao, L.; Zhao, X. *J. Appl. Polym. Sci.* **2004**, *94*, 2517.
16. Liu, B.; Shaw, M. T. *J. Rheol.* **2001**, *45*, 641.
17. Chakraborti, P.; Toprakci, H. A. K.; Yang, P.; Spigna, N. D.; Franzon, P.; Ghosh, T. *Sens. Actuators A* **2012**, *179*, 151.
18. Hong, X.; Midori, T.; Toshihiro, H. *Sens. Actuators A* **2010**, *157*, 307.
19. Ludeelerd, P.; Niamlang, S.; Kunaruksapong, R.; Sirivat, A. *J. Phys. Chem. Solids* **2010**, *71*, 1243.
20. Hao, L.; Shi, Z.; Zhao, X. *React. Funct. Polym.* **2009**, *69*, 165.
21. Hao, L. M.; Ding, C. L.; Zhao, X. P. *J. Appl. Polym. Sci.* **2011**, *119*, 2991.
22. Yin, J. B.; Zhao, X. P. *Chem. Mater.* **2002**, *14*, 4633.
23. Krause, S.; Bohon, K. *Macromolecules* **2001**, *34*, 7179.
24. Gao, L. X.; Zhao, X. P. *J. Appl. Polym. Sci.* **2007**, *104*, 1738.
25. Gao, L. X.; Zhao, X. P. *Int. J. Mod. Phys. B* **2005**, *19*, 1449.
26. Wang, B.; Rozynek, Z.; Zhou, M. *J. Phys. Conf. Ser.* **2009**, *149*, 1.
27. Tungkavet, T.; Seetapan, N.; Pattavarakorn, D.; Sirivat, A. *Mater. Sci. Eng. C* **2014**, *46*, 281.
28. Huang, H.; Wu, J.; Lin, X.; Li, L.; Shang, S.; Yuen, M. C.; Yan, G. *Carbohydr. Polym.* **2013**, *95*, 72.
29. Zhang, J.; Wang, L.; Wang, A. *Ind. Eng. Chem. Res.* **2007**, *46*, 2497.
30. Michael, Z.-C. H.; Kurian, V.; Andrew, E. P.; Claudia, J. R.; Rodney, D. H. *Powder Technol.* **2000**, *110*, 2.
31. Poon, L.; Wilson, L. D.; Headley, J. V. *Carbohydr. Polym.* **2014**, *109*, 92.
32. Gao, L.; Li, L.; Qi, X.; Wei, W.; Hai, J.; Gao, W.; Gao, Z. *Polym. Compos.* **2013**, *34*, 897.
33. Adireddy, S.; Lin, C. K.; Cao, B. B.; Zhou, W. L.; Caruntu, G. *Chem. Mater.* **2010**, *22*, 1946.
34. Zhao, H. P.; Liu, Z. Y.; Liu, Y. Y. *Phys. B* **2001**, *299*, 64.